Modelling a Calcium-Looping Fluidised Bed Calcination Reactor with Solar-Driven Heat Flux

Mayra Alvarez Rivero[a], Diogo Rodrigues[a], Carla I.C. Pinheiro[a,*], João P. Cardoso[b],
L. Filipe Mendes[c]

[a] Centro de Química Estrutural, Instituto Superior Técnico, Universidade de Lisboa, Av. Rovisco Pais 1, 1049-001 Lisboa, Portugal
[b] Laboratório Nacional de Energia e Geologia, I.P., Estrada do Paço do Lumiar 22, 1649-038 Lisboa, Portugal
[c] IN+/LARSyS, Instituto Superior Técnico, Universidade de Lisboa, Av. Rovisco Pais 1, 1049-001 Lisboa, Portugal
 carla.pinheiro@tecnico.ulisboa.pt

A new unidimensional computational model is developed to simulate a calcination reactor in a Calcium-looping process for thermochemical energy storage in concentrating solar power systems. The proposed reactor is an absorber tube exposed to concentrated solar radiation. This tube is also the riser of a circulating fluidised bed where the calcination reaction takes place. The proposed heat transfer process models are based on the core-annulus model and the hydrodynamic model is a modified version of the Kunii-Levenspiel model. The model considers the change in the mass flow rate of species and the density change of the phases in the axial direction of the reactor, usually considered constant in the models found in the literature. A higher calcination efficiency, up to 8 p.p., is obtained for the studied reference case when assuming constant density and mass flow rate. Simulations were performed by imposing a solar-driven non-uniform heat flux distribution on the reactor wall. The results show that a 6 m height reactor allows achieving a calcination efficiency of 66% for the reference conditions used. A sensitivity analysis shows that the solids mass flow rate and the inlet bed temperature are the parameters that most affect the calcination process efficiency.

1. Introduction

Concentrating solar power (CSP) is unique among the renewable energy technologies because it can easily be coupled with thermal energy storage (TES), making it highly dispatchable. Nowadays commercial TES uses molten-salt technology, which accounts for 75 % of the globally installed TES capacity. However, the molten salts that are currently used as heat transfer fluid have several disadvantages: corrosiveness, the maximum working temperature (~560 °C), which limits the system efficiency, and the significant energy consumption required to keep the molten salts at temperatures over 220 °C, to avoid solidification (Ortiz et al., 2019). In contrast, thermochemical energy storage (TCES) is an option that allows higher energy densities (Lovegrove and Stein, 2012). Several reversible reactions have been proposed for TCES, mainly based on carbonates, hydroxides, metal redox, and hydrides. One of the most promising systems relies upon the calcination-carbonation reversible reaction of $CaCO_3$-CaO and is known as the Calcium-looping (CaL) process. In this system, concentrated solar radiation is used to carry out the endothermic calcination reaction:

$$CaCO_3(s) \Leftrightarrow CaO(s) + CO_2(g), \qquad \Delta H_{calc} = 178.4 \times 10^3 \, \text{J mol}^{-1} \tag{1}$$
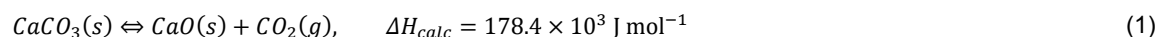
The reaction products CaO and CO_2 may be stored separately and, when needed, they are brought together to carry out the exothermic carbonation reaction, releasing the stored energy (Ortiz et al., 2019). The main advantages of the CaL process are: (i) the low cost, wide availability, and harmlessness of natural CaO precursors, such as limestone and dolomite, (ii) the theoretical energy density of the CaL system, which is one of the largest among TCES systems, and (iii) the high reaction temperature of carbonation, which can overcome the current CSP temperature limitations of 550 to 600 °C for molten salts.

The CaL process for post-combustion CO_2 capture has been successfully demonstrated at lab- and pilot-scale, with carbonation under low CO_2 concentration and calcination under high CO_2 concentration at temperatures

around 850-950 °C. However, CaL conditions for TCES may differ since the concentration of CO_2 entering the carbonator is not imposed and can be selected to increase the efficiency of the power cycle (Ortiz et al., 2019). Despite the importance of solar calciners in the CaL process for TCES, no consensus exists regarding a reactor model that encompasses the effects of reaction kinetics, hydrodynamics, heat transfer, and concentrated solar radiation. This is particularly true when the reactor is a continuous circulating fluidised bed (CFB), even though this configuration provides high heat and mass transfer rate, good mixing of solids, and adjustable residence time with long permanence in high-temperature zones. Hence, the main goal of this study is to address this gap in the literature by developing a model of a continuous CFB for solar calcination of $CaCO_3$. The proposed model describes the reaction kinetics, hydrodynamics, and heat transfer in the reactor for the case of non-uniform heat flux distribution, including the effect of the changes in mass flow rate and density due to the chemical reaction. A sensitivity study is performed to identify the most important parameters affecting the reactor efficiency.

2. Reactor model

The proposed reactor configuration is a continuous CFB, consisting of an absorber tube, which has the role of a riser of the CFB, the walls of which are exposed to concentrated solar radiation, allowing indirect heating of the reaction chamber. The selection of the operating conditions for the proposed CFB reactor is based on existing CaL lab-scale and pilot-scale calciners which are usually designed for low solids fluxes, below 30 kg m^{-2} s^{-1}, and superficial gas velocities varying from 1.5-6 m s^{-1}. These calciners fall in the low-density CFB region (Sun and Zhu, 2019), thus the calciner of this model is designed for the fast fluidisation regime. In a fast fluidised bed, two regions are encountered: the dense zone, which corresponds to the lower part of the riser with an almost constant volumetric fraction of solids in the order of 0.15-0.22, and the lean zone, which is the following zone where solids are entrained, and the solids volumetric fraction decreases progressively (Kunii and Levenspiel, 1991). In the lean zone, the flow is described by a core-annulus flow pattern. The cross-section of the lean zone is further divided into two regions: a dilute core with bed particles transported upwards by the fluidising gas, and a dense and smaller annulus region where clusters flow down over the reactor wall. After travelling a certain distance, the clusters dissolve and detach themselves from the wall to be re-entrained into the core region where they mix with fresh particles at the bed temperature.

2.1 Model assumptions

For the implementation of the proposed mathematical model, several assumptions are made: (a) the diffusivity terms are neglected; (b) the reactor is at steady state; (c) the static pressure due to the particles is neglected; (d) the gas species are ideal gases; (e) in the dense zone and in each element of the lean zone, the thermophysical properties of the species are constant; (f) the solids volumetric fraction in the lean zone is described by an adaptation of the K-L model (Kunii and Levenspiel, 1991); (g) the velocity of all the gas species is the same, and the velocity of all the solid species is the same; (h) the heat transfer in the lean zone is described by a core-annulus model; (i) the heat transfer between the reactor wall and the fluidised bed is modelled with a total heat transfer coefficient (HTC) for each element; (j) the solids and the gas are in thermal equilibrium; (k) the energy of the flow is due to its enthalpy only.

2.2 Mass conservation model equations

The total mass balances for the solid species as a function of the axial position z (m) are:

$$\frac{d\dot{m}_i(z)}{dz} = \nu_i M_i c_s(z) k_{calc}(z) X_{CaCO_3}(z)^{2/3}\left(c_{CO_2,eq}(z) - c_{CO_2}(z)\right)A, \qquad i \in \{CaCO_3, CaO\} \tag{2}$$

where $\dot{m}_i$ is the mass flow rate of the species i (kg s^{-1}), ν_i is the stoichiometric coefficient in the calcination reaction (-), M_i is the molar mass (kg mol^{-1}), X_i is the molar fraction (-), c_s is the total number of moles of the solid components per unit of volume reactor (mol m^{-3}), c_{CO_2} is the local concentration of CO_2 (mol m^{-3}), and A is the cross-section area (m^2). The kinetic constant k_{calc} of $CaCO_3$ calcination (m^3 mol^{-1} s^{-1}) and the equilibrium concentration $c_{CO_2,eq}$ of CO_2 (mol m^{-3}) are the ones proposed by Martínez et al. (2013) and Fang et al. (2009). The mass flow rate of CO_2 (kg s^{-1}) can be obtained by mass conservation:

$$\dot{m}_{CO_2}(z) = \dot{m}_{CO_2}(0) + \dot{m}_{CaO}(0) + \dot{m}_{CaCO_3}(0) - \dot{m}_{CaO}(z) - \dot{m}_{CaCO_3}(z) \tag{3}$$

The solids concentration and the local concentration of CO_2 are described by:

$$c_s(z) = \left(\dot{m}_{CaO}(z)/M_{CaO} + \dot{m}_{CaCO_3}(z)/M_{CaCO_3}\right)/(U_s(z)A) \tag{4}$$

$$c_{CO_2}(z) = \left(\dot{m}_{CO_2}(z)/M_{CO_2}\right)/\left(U_g(z)A\varepsilon_g(z)\right) \tag{5}$$

where U_s and U_g are the velocities of the solid and gas phases (m s^{-1}) and ε_g is the gas volumetric fraction (-).

2.3 Hydrodynamic model

The solids volumetric fraction ε_s (-) is described by the K-L model from Kunii and Levenspiel (1991) for the dense and lean zones in the riser:

$$\varepsilon_{s,lean}(z) = \varepsilon_s^* + \left(\varepsilon_{s,dense} - \varepsilon_s^*\right)e^{-a\,(z-H_{dense})} \tag{6}$$

where the subscripts $lean$ and $dense$ denote the lean and dense zones in the riser, ε_s^* is the saturation carrying capacity (-), a is the decay factor (m^{-1}), and H_{dense} is the height of the dense bed (m). The solids volumetric fraction $\varepsilon_{s,dense}$ in the dense zone (-) is computed from a correlation (Kunii and Levenspiel, 1991).

For cold columns without reactions and with constant solids and gas mass flow rates along z, the changes of velocities are due to the changes of volumetric fractions only. The gas velocity starts at its maximum and the solids velocity starts at its minimum. They change monotonically and meet at the pneumatic transport conditions. When the gas mass flow rate and temperature increase, the gas velocity also increases. Hence, the K-L model is adapted to take these factors into consideration. The increase of gas velocity for the saturated carrying capacity condition implies a smaller saturation carrying capacity than the one expected from the K-L model. The asymptotic value of solids volumetric fraction can be found for the conditions where solids and gas have the same velocity and complete calcination has been achieved. For a cold fluidised bed, this would be sufficient, but for this model the adopted approach for the saturation carrying capacity is to choose a suitable value to be used in the simulations based on testing different bed temperatures (in the range 650-1000 °C) in equilibrium with the wall. The decay factor is related to the values of the volumetric fraction in a short initial part of the lean zone. It is found in the literature as depending on the superficial gas velocity U_0 (m s^{-1}), which is the velocity that the gas would have if it occupied the whole section of the reactor. A range of experimental values of a was presented by Kunii and Levenspiel (1991) for operating conditions similar to the ones in this study, although with constant mass flow rates. Based on those results, a lies in the interval $\left[\frac{4}{U_0}; \frac{12}{U_0}\right]$ m^{-1}. In this model, the pneumatic transport conditions may be reached before the reactor outlet. The model assumes that pneumatic transport starts as soon as the solids and gas velocities are equal.

2.4 Energy conservation model equations

The bed temperature T_b (K) can be obtained from an energy conservation balance, based on the powers per unit of length $\widetilde{H}_{calc}$ and $\widetilde{H}_{wall-bed}$ for the reaction kinetics and heat transfer from the walls (W m^{-1}), respectively:

$$\frac{dT_b(z)}{dz} = \frac{1}{\sum_i \dot{m}_i(z)C_{P_i}(z)}\left(\widetilde{H}_{wall-bed}(z) - \widetilde{H}_{calc}(z)\right) \tag{7}$$

$$\widetilde{H}_{calc}(z) = \Delta H_{calc}c_s(z)k_{calc}(z)X_{CaCO_3}(z)^{2/3}\left(c_{CO_2,eq}(z) - c_{CO_2}(z)\right)A \tag{8}$$

$$\widetilde{H}_{wall-bed}(z) = h_{w-b}(z)\,\pi\,D\,(T_w(z) - T_b(z)) \tag{9}$$

where the subscript i refers to each solid and gas species with specific heat capacity C_{P_i} (J kg^{-1} K^{-1}), D is the reactor diameter (m), T_w is the wall temperature (K), and h_{w-b} is the total HTC (W m^{-2} K^{-1}).

From experiments in CFB risers, it is known that the walls of the riser are intermittently washed by clusters and a dilute gas-solid stream (Rusheljuk, 2006). Different heat transfer mechanisms are involved: (1) convection/conduction between clusters and wall through a thin gas film, (2) radiation from clusters, (3) convection, and (4) radiation from the disperse phase. A total HTC is computed by summing up the individual heat transfer mechanisms while considering the fraction δ_c of the wall in contact with clusters (-) while the rest is in contact with the dilute gas-solid stream. The total HTC between the surface and the fluidised bed is:

$$h_{w-b}(z) = \delta_c(z)(h_c(z) + h_{c,rad}(z)) + (1 - \delta_c(z))(h_{d,con}(z) + h_{d,rad}(z)) \tag{10}$$

where the subscripts $c, d, con,$ and rad refer to the HTC for the cluster phase, disperse phase, convection, and radiation (W m^{-2} K^{-1}), respectively. The time-averaged fraction δ_c of the wall area covered by the clusters may be estimated from the gas volumetric fraction within the clusters and near the wall (Li et al., 1988).

The wall is in contact with the upflowing disperse phase in the space between two clusters. The HTC from a dilute uniform suspension of a gas-solid mixture is given by an approximation proposed by Basu (2015) based on the particle diameter, thermal conductivity, specific heat capacities of gas and solids, and terminal velocity of particles, as well as the density of the disperse phase and Prandtl number that depend on the solid volumetric fraction of the disperse phase in the vicinity of the wall. The HTC of the radiation from the disperse phase to the

wall is computed based on the wall emissivity and the effective emissivity of a particle cloud considering scattering, where the bed emissivity is calculated from the emissivity of the particle surface (Brewster, 1986). The clusters are assumed to travel a certain distance, move away from the wall, disintegrate, and reform periodically in the riser (Rusheljuk, 2006). While the cluster is in contact with the wall, it initially has the bed temperature. After that, a transient heat transfer between the wall and the cluster occurs. The heat transfer from the cluster involves both the contact resistance on the wall and the conduction resistance of the cluster. The contact resistance corresponds to the thermal resistance offered by a gas film of a thickness that is a fraction of the particle diameter (Basu, 2015). Then, the HTC from the cluster to the wall is given as a function of the particle diameter, average residence time of clusters on the wall, thermal conductivity of gas evaluated at the mean gas-film temperature, and several cluster properties, such as thermal conductivity, volumetric fraction, specific heat capacity, and density. The HTC of the radiation from the clusters to the wall is computed based on the emissivity of clusters considering multiple reflections of particles (Grace, 1984), as well as the cluster temperature and the average suspension density (Dutta and Basu, 2004).

3. Results

The reactor diameter and height were selected based on the literature review of current lab-scale CaL systems. Values of 0.1 m diameter and 10 m height were selected as a reference for design, and the final height is recommended based on the simulation results. The riser wall was assumed to be of stainless steel with an emissivity of 0.8. The pressure chosen for the reference case was 1.2×10^5 Pa. The densities of the solids were obtained from laboratory measurement using a sample of sorbent with a particle diameter in the range of 250-350 µm. The particle diameter selected for the reference case was 300 µm. The height of the dense bed was selected as 0.25 m for the reference case, after reviewing available experimental data from low-density CFBs. A reference value of $\frac{4}{U_0}$ m^{-1} for the decay factor was chosen for this study, and the range $\left[\frac{4}{U_0}; \frac{12}{U_0}\right]$ m^{-1} was tested. A reference value of 2×10^{-4} was used for the solids fraction at saturated carrying capacity since it is almost constant in a temperature interval of 650-1000 °C. The solids circulation rate and the superficial gas velocity ranged from 0.6-5 kg m^{-2} s^{-1} and 2-6 m s^{-1} in the reviewed calciners. This translates into solids and gas flow rates on the order of 0.02 kg s^{-1}, which was selected as the reference value. The inlet mass fractions of CaO in the solid phase (0.05) and CO_2 in the gas phase (0.2) were also selected according to typical experimental conditions found in the literature. The bed temperature at the inlet was assumed to be 650 °C as this is the typical temperature at the outlet of the carbonator in CaL processes (Teixeira et al., 2019). For TCES in CSP systems, this temperature may be lower depending on the storage conditions for the carbonation products. To characterise the reactor performance, the calcination molar efficiency η (-) is defined as the fraction of $CaCO_3$ calcined in the reactor:

$$\eta \equiv 1 - X_{CaCO_3}(H_t)/X_{CaCO_3}(0) \tag{11}$$

where H_t is the total height of the reactor (m). The results for constant wall temperature and non-uniform heat flux distribution, including sensitivity analysis, are presented in detail in the work of Alvarez Rivero (2021).

If constant densities and constant mass flow rates were assumed, as considered by several authors in the literature, this would lead to an overestimation of the calcination efficiency of 5 p.p. and 8 p.p. for 6 m and 10 m height, respectively. A non-uniform heat flux distribution along the vertical axis of the tube was used to model the concentrated solar radiation. The solar flux is modelled as the sum of 2 Gaussian distributions that replicates a multiple aiming point strategy (heat flux $H_{wall-bed}$ in Figure 1a). The total HTC varies from 200-400 W m^{-2} K^{-1}. These values are in the range of the values reported in the literature. The calcination heat flux shows that the reaction starts at 1.3 m (heat flux H_{calc} in Figure 1a). This height corresponds to the point where the CO_2 equilibrium concentration surpasses the local CO_2 concentration. After several tests to change the heat flux distribution, the efficiency varied from 0.5 to 0.7. However, the bed temperature always reached 900 °C around 5 m height (Figure 1b). Temperatures above this value should be avoided due to the strong increase of the sintering process. The mass flow rates become constant after 6 m height (Figure 2a for the gas and Figure 2b for the solids). The calcination efficiency at 6 m and 10 m height is 0.66 and 0.70, which means that little improvement is achieved after 6 m. However, this is a result of the flux distribution, which approaches zero around that height. After 6 m height, the calcination proceeds at the expense of the internal energy of the bed. In the sensitivity study, the effect of the model parameters and operating conditions was evaluated. It was found that the only conditions with a strong effect on the calcination efficiency are the solids mass flow rate and the inlet bed temperature. The reason for the negligible effect of the other parameters could be the distribution of the imposed heat flux since its peak is concentrated on the first half of the reactor, while after 5 m it decreases dramatically to reach zero. The decrease of the mass flow rate of solids has a significant effect, with 47 p.p. of improved efficiency. For low mass flow rate, complete calcination is achieved (Figure 3a). For the used flux

distribution, it was not possible to calcine $CaCO_3$ with an initial bed temperature at 25 °C (Figure 3b). The flux distribution is not enough to provide the power needed to heat the bed up to a temperature at which calcination can proceed (Figure 3c). The inlet bed temperature strongly affects the calcination efficiency. For a temperature of 25 °C, the efficiency decreases by 68 p.p. with respect to the reference case with a temperature of 650 °C.
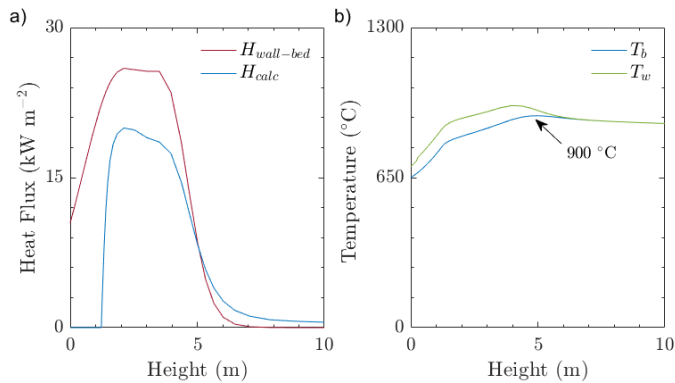
Figure 1: Distribution along the axial direction of the calciner of a) wall-to-bed and calcination heat fluxes and b) temperature profiles of the bed and wall
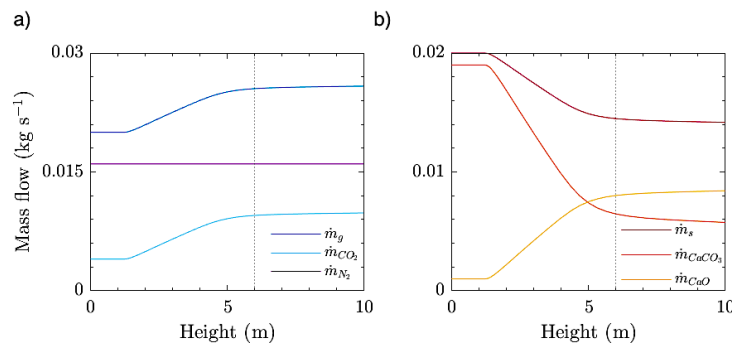
Figure 2: Distribution along the axial direction of the calciner of mass flow rates of a) gas and b) solid species
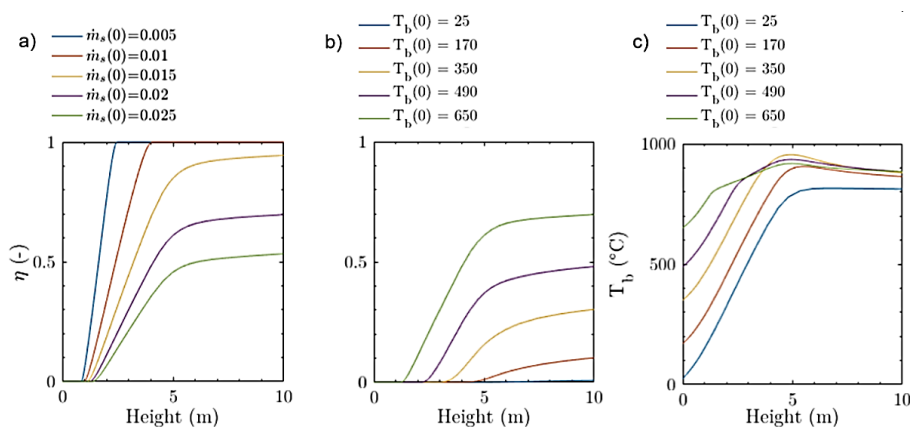

Figure 3: Sensitivity study for the effects of a) mass flow rate of the gas, and b, c) inlet bed temperature

4. Conclusions

A novel unidimensional, steady-state computational model coupling heat transfer, hydrodynamics, and chemical reaction kinetics is presented for a solar calcination reactor for TCES in CSP systems. The reactor consists in an absorber tube exposed to concentrated solar radiation, where the tube is also the riser of a CFB where the calcination reaction proceeds. The proposed model uses the calcination reaction kinetics proposed by Martínez

et al. (2013), the core-annulus heat transfer models, and a modified version of the K-L model. The original K-L model was modified to account for the gas generated by the chemical reaction and the change in bed temperature. With the proposed model, it was verified that the usual assumption of constant temperature and constant mass flow rate leads to an overestimation of the calcination efficiency up to 8 p.p.. The model was implemented for the case of non-uniform heat flux distribution representing the effect of concentrated solar radiation. A fraction of the reactor height, 1.3 m, is needed for heating the gas up to a point where the CO_2 equilibrium concentration surpasses its local concentration. The required reactor height under the reference conditions is around 6 m since the mass flow rates become constant and no significant improvement in the efficiency is achieved for larger heights. The calcination efficiency at 6 m height is 0.66.

A sensitivity study was performed to analyse the effect of the inlet conditions and some model parameters. The decrease of the solids mass flow rate and of the inlet bed temperature cause the strongest effects on the calcination efficiency (47 p.p. increase and 68 p.p. decrease, respectively). The calcination reaction does not proceed when the inlet bed temperature is 25 °C, which shows the importance of preheating the gas-solid flow. The results obtained show that the developed model is a promising tool that allows distinguishing critical issues to be considered while designing new solar reactors for CaL, such as the aiming strategy for the solar radiation and the temperature control required to avoid sintering above 900 °C. The simplicity and fast computation time allow the user to obtain quick results while testing how different parameters affect the reactor performance.

In future work, this model will be coupled with the receiver cavity model and the CSP field, which will allow testing different configurations, such as several risers inside the receiver cavity.

Acknowledgements

References

Alvarez Rivero M., 2021, Modeling a Circulating Fluidized Bed $CaCO_3$ Calcination Reactor for Thermochemical Energy Storage in a Concentrating Solar Power System, MSc Thesis, Instituto Superior Técnico, Universidade de Lisboa, Lisboa, Portugal.

Basu P. (Ed), 2015, Circulating Fluidized Bed Boilers, Springer, Cham, Switzerland.

Brewster M.Q., 1986, Effective absorptivity and emissivity of particulate media with application to a fluidized bed, Journal of Heat Transfer, 108, 710–713.

Dutta A., Basu P., 2004, An improved cluster-renewal model for the estimation of heat transfer coefficients on the furnace walls of commercial circulating fluidized bed boilers, Journal of Heat Transfer, 126, 1040–1043.

Fang F., Li Z.S., Cai N.S., 2009, Experiment and modeling of CO_2 capture from flue gases at high temperature in a fluidized bed reactor with ca-based sorbents, Energy and Fuels, 23, 207–216.

Grace J.R., 1984, Hydrodynamics of Gas Fluidized Beds, Chapter In: Basu P. (Ed), Fluidized Bed Boilers, Pergamon Press, Willowdale, ON, Canada, 13–30.

Kunii D., Levenspiel O., 1991, High-velocity Fluidization, Chapter In: Kunii D., Levenspiel O. (Eds), Fluidization Engineering, Butterworth-Heinemann, Newton, MA, USA, 193–210.

Li J., Tung Y., Kwauk M., 1988, Energy Transport and Regime Transition in Particle-Fluid Two-Phase Flow, Chapter In: Basu P., Large J.F. (Eds), Circulating Fluidized Bed Technology II, Pergamon Press, Oxford, UK, 75–87.

Lovegrove K., Stein W. (Eds), 2012, Concentrating Solar Power Technology: Principles, Developments and Applications, Woodhead Publishing, Sawston, UK.

Martínez I., Grasa G., Murillo R., Arias B., Abanades J.C., 2013, Modelling the continuous calcination of $CaCO_3$ in a Ca-looping system, Chemical Engineering Journal, 215–216, 174–181.

Ortiz C., Valverde J.M., Chacartegui R., Perez-Maqueda L.A., Giménez P., 2019, The Calcium-Looping ($CaCO_3$/CaO) process for thermochemical energy storage in Concentrating Solar Power plants, Renewable and Sustainable Energy Reviews, 113, 109252.

Rusheljuk P., 2006, Heat Transfer in Circulating Fluidized Bed, <egdk.ttu.ee/files/kuressaare2006/Kuressaare2006_167Rusheljuk.pdf > accessed 11.06.2021.

Sun Z., Zhu J., 2019, A consolidated flow regime map of upward gas fluidization, AIChE Journal, 65, 1–15.

Teixeira P., Hipólito J., Fernandes A., Ribeiro F., Pinheiro C.I.C., 2019, Tailoring synthetic sol–gel CaO sorbents with high reactivity or high stability for Ca-looping CO_2 capture, Industrial and Engineering Chemistry Research, 58, 8484–8494.